Pergamon

*Journal of Structural Geology*, Vol. 16, No. 4, pp. 447 to 466, 1994

0191-8141/94 $6.00 + 0.00

0191-8141(93)E0002-3

# Strain and vorticity patterns in ideally ductile transpression zones

PIERRE-YVES F. ROBIN and ALEXANDER R. CRUDEN

Tectonic Studies Group, Geological Sciences, Erindale Campus, University of Toronto, Mississauga, Ontario, Canada L5L 1C6

(*Received* 3 *February* 1993; *accepted in revised form* 14 *October* 1993)

**Abstract**—The prevalent model for ductile shear zones assumes that they develop by progressive simple shearing, resulting in a monoclinic fabric in which the vorticity vector is parallel to the shear zone and perpendicular to the lineation. But some ductile shear zones exhibit an amount of coaxial flattening, or a fabric pattern which appear to be incompatible with the assumptions of plane strain and progressive simple shear. In certain sections of the Archean Larder Lake–Cadillac deformation zone (LCDZ), for example, vorticity indicators (asymmetric pressure wings, Z-folds, *S*–*C* fabrics), best seen on horizontal surfaces, indicate dextral transcurrent motion, whereas stretching lineations have variable but steep plunges. In the Proterozoic Mylonite Zone (MZ) of south-west Sweden, vorticity indicators combined with foliation and lineation data suggest a continuous change from reverse dip-slip motion close to the footwall to sinistral transcurrent motion adjacent to the hangingwall of the zone. Such departures from the ideal progressive simple shear zone pattern may in fact be common. Rather than invoke two stages of deformation, we explore the possibility that these patterns could be the result of ductile transpression.

Ductile transpression between relatively rigid walls implies an extrusion of material out of the shear zone. When the material cannot slip freely along the boundaries of the zone, the extrusion strain is by necessity heterogeneous. In order to explore these heterogeneous strain distributions, we have developed a continuum mechanics model in which the 'transpressed' rock is a linear viscous material squeezed upward between two parallel, rigid, vertical walls. Transpression is further generalized by modelling oblique (i.e. with a dip-slip component) relative displacements of the walls. Models, which can vary in their obliquity and their 'press'/'trans' ratio, are examined for their distributions of *K*-values, strain rate intensity, 'lineation' (direction of maximum principal strain rate), 'foliation' (plane perpendicular to the direction of minimum principal strain rate) and vorticity. To quantify the expected petrographic effect of the vorticity when the strain path has triclinic symmetry, we introduce a sectional kinematic vorticity number, $W_k^s$.

The model predicts 'foliations' and 'lineations' which vary in orientation and intensity across the zone. In some model zones, the vorticity vector can be nearly parallel to the 'foliation' and perpendicular to the 'lineation', as expected in progressive simple shear, but it can also be locally nearly parallel to the 'lineation', as in the LCDZ. Commonly, however, the vorticity vector is not parallel to any of the principal directions of instantaneous strain, and the deformation has triclinic symmetry. The pattern of foliations and lineations in the MZ can readily be matched to that in an oblique transpression model zone.

## INTRODUCTION

TRANSPRESSION is a popular concept for interpretation of both shallow-level deformation zones (e.g. San Andreas, see Sylvester & Smith 1976, Bürgmann 1991) and ductile shear zones (e.g. the Archean Quetico Belt, see Hudleston *et al.* 1986, 1988, Borradaile *et al.* 1988; other Archean subprovinces of the Superior Province, see Stott *et al.* 1987; Caledonides, see Hanmer 1981 for Newfoundland, Hutton 1987 for the British Isles, Ratliff *et al.* 1986 for Spitzbergen; late Precambrian Cadomian Belt, see D'Lemos *et al.* 1992). One may in fact distinguish two related, but distinct, meanings of transpression in geology. The first meaning, which we might describe as its regional tectonic meaning, simply refers to the relative displacement of two regions of the lithosphere moving with respect to each other in combined convergent and transcurrent motion (Harland 1971); the tectonician is only accessorily concerned with the way in which rocks actually accommodate this imposed relative displacement of the two regions. For example, a combination of motions along thrust and strike-slip faults, or oblique motions along thrust faults which are neither vertical nor horizontal may be sufficient to demonstrate transpression in its tectonic sense (e.g. Ratschbacher 1986). The thrust component of regional transpression requires a thickening of the region affected by transpression, accompanied by either simultaneous or later erosion.

A second meaning, which might be labelled 'structural', was apparently introduced by Harland (1971), and later kinematically modelled by Sanderson & Marchini (1984). Transpression, in this structural sense, refers to what specifically happens to a tabular zone of rocks submitted to the boundary conditions shown in Fig. 1: a planar zone (usually steeply dipping) of rock is submitted by its walls to a simultaneous flattening (the 'press' component of transpression) and shearing (the 'trans' component). There results a 'room problem', because the planar shear zone is confined at its base and laterally. This room problem can only be overcome by volume loss or by extruding the material upward (Fig. 1). We are concerned here with this 'structural' meaning of transpression.

In Sanderson & Marchini's (1984) and Sanderson & McCoss's (1991) models, the material in the zone does not change volume but escapes by freely slipping along the zone walls in the vertical direction (Fig. 1a). In that model (which we shall refer to as the Sanderson and Marchini transpression zone, or SMTZ), the internal

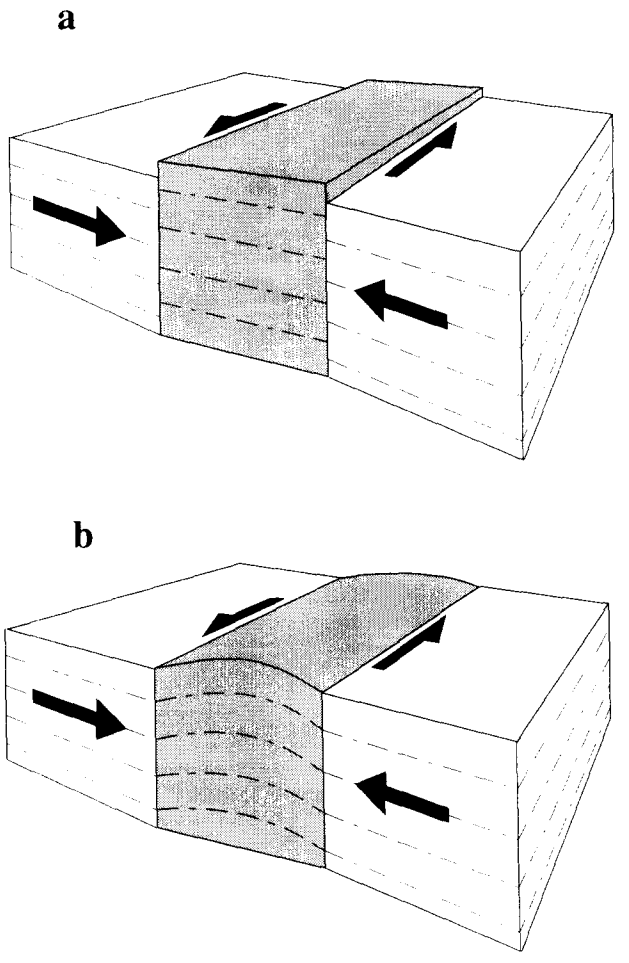


Fig. 1. Transcurrent ductile transpression of a planar deformation zone (shaded). Dotted lines represent the trace of originally horizontal and continuous marker horizons. (a) Sanderson & Marchini's (1984) model in which material at the boundaries of the zone is allowed to slip freely in the vertical direction while adhering perfectly in the horizontal direction. The resulting velocity field is uniform and strain is homogeneous throughout the zone. (b) Ductile transpression with a no-slip condition at the zone boundaries as modelled in this study. Unlike (a) the velocity field is now approximately parabolic and the strain within the zone is heterogeneous.

flow and strain is uniformly distributed across the zone and the *vorticity vector* is always vertical. But, as Sanderson & Marchini (1984) pointed out, sufficient values of the flattening component across the zone also cause a vertical stretching lineation. It is this departure from the symmetry of usual progressive simple shear which we want to examine with more realistic models of transpression zones.

Objections to the SMTZ model were already mentioned by Sanderson and Marchini themselves, and discussed by subsequent authors. An important mechanical objection is that the model requires that the boundaries of the shear zone have strange and unlikely frictional properties (Schwerdtner 1989). These boundaries are assumed to be free slipping in the vertical direction, i.e. assumed to support no vertical shear stress, since the material is homogeneously strained during its extrusion. But at the same time these boundaries must not allow slip in the horizontal direction, i.e. they must transmit horizontal shear stress, so that the transcurrent shear can be imposed on the material in the zone (Schwerdtner 1989). Such boundaries could indeed be implemented in a physical model, with the rigid walls consisting of perfectly lubricated vertical corrugations; the perfect lubrication would offer no resistance to the extrusion component of the motion, but the corrugations would transmit the horizontal shear stress. In actual ductile domains, however, the presence of the two bounding faults, with or without these anisotropic frictional characteristics, has not been reported as a result of transpression.

In this study, we develop models of transpression zones in which the material within the zone does not slip freely along the wall of the zone, in any direction (Fig. 1b). It is in principle possible to generate strictly kinematic displacement field models in which the only requirement is to satisfy the displacement conditions at the boundaries of the zone. Schwerdtner (1989) had concluded that the kinematic treatment of transpression may be insufficient and that a dynamical treatment may be required, and we indeed found it preferable, and as it happens easier, to obtain full continuum mechanics solutions to the same boundary value problem. These solutions, which thus satisfy both the requirement of strain compatibility and that of mechanical equilibrium everywhere, avoid a common concern with strictly kinematic models, which is that they may be mechanically impossible or unrealistic. The material within the zone is modelled as linearly viscous, and we only deal with strain rates, which permits the use of the principle of superposition and makes the solutions particularly easy to obtain. We believe that many features of our results are quite robust, and do not depend on rocks being truly linearly viscous. Some of the results for the case of transcurrent shear, illustrated in Fig. 1(b), have already been presented (Robin & Cruden 1991), but we present here the theory for the more general case of oblique shear, i.e. when the shear has both strike-slip and dip-slip components, and we compare the predicted patterns to field examples.

A feature of all our solutions to the transpression problem is that the symmetry of the deformation at many points is triclinic, rather than monoclinic. That is, the vorticity vector is not parallel to any one principal direction of the symmetric strain tensor. We have not found in the geological literature any extensive discussion of triclinic deformation, but it is possible, even likely, that triclinic deformation symmetry is common in nature. Although we do not speculate on the petrographic expression of triclinic deformation, we propose, and calculate for our model, a 'sectional' kinematic vorticity number, $W_k^s$, to quantify an expected petrographic expression of the vorticity.

## TWO POSSIBLE EXAMPLES OF TRANSPRESSION ZONES

Transpressive regimes have been proposed for several domains deformed under mesozonal conditions, and we describe below two such areas, both from Precambrian

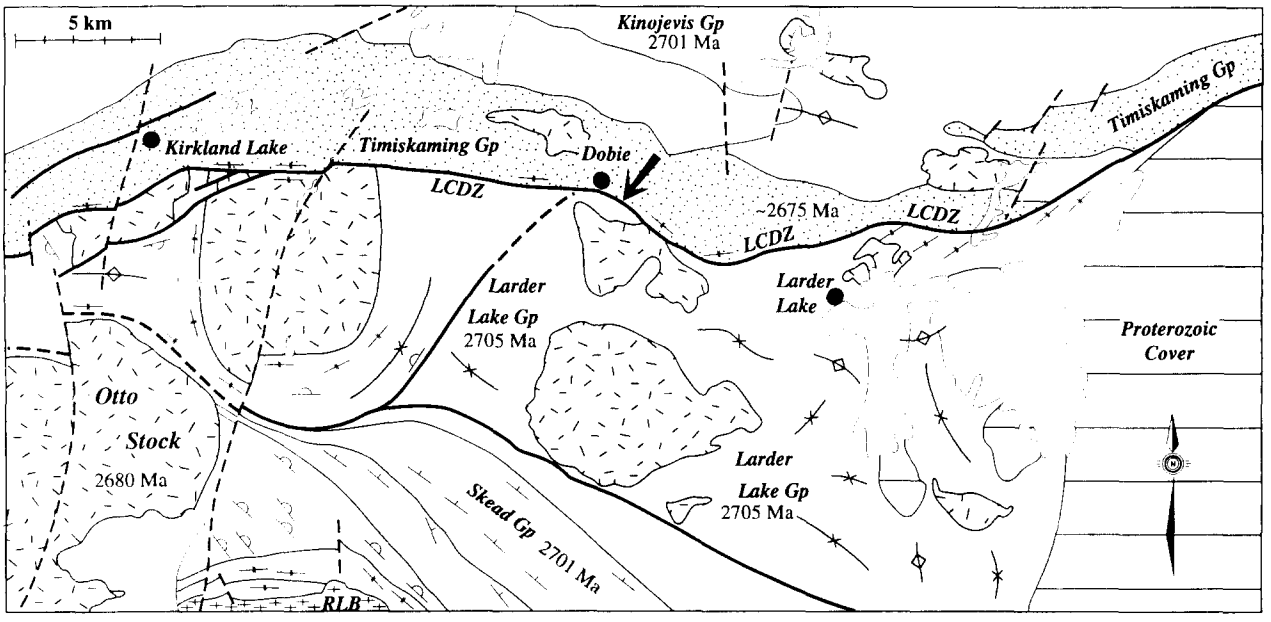


Fig. 2. Geology and major structures of the Kirkland Lake area (after Jensen 1985). Syenitic plutons: hachured pattern. Timiskaming Group metasediments and metavolcanics: dotted pattern. LDCZ = Larder Lake–Cadillac deformation zone. Arrow points to locations of photographs in Fig. 4.

shields. We present important features of the distribution of their strain fabrics in order to compare them with the predictions of our models.

*The Archean Larder Lake–Cadillac break*

Transpression has been proposed for many of the E–W-trending subprovince and intraprovince boundaries of the Archean Superior Province (Stott *et al.* 1987, Williams *et al.* 1991). Common characteristics of such zones include: subvertical transposition foliations; upright folds oblique to zone boundaries; non-plane (flattening) strains; the presence of shear-sense indicators on sub-horizontal surfaces; and mineral/shape (i.e. stretching) lineations which vary from subhorizontal (e.g. Quetico-Shebandowan, see Borradaile & Spark 1991, Hudleston *et al.* 1988) to subvertical (e.g. Larder Lake–Cadillac deformation zone, see Robert 1989). Dextral transpression has been proposed in all of these studies, with synchronous, approximately N–S shortening and nearly E–W dextral shear (Borradaile & Spark 1991).

The Larder Lake–Cadillac deformation zone (LCDZ, Fig. 2) is a major (>300 km long), E–W-trending, Au-bearing, intraprovince boundary within the Abitibi subprovince of the Archean Superior Province (Jackson & Fyon 1991). In the Kirkland Lake area (Fig. 2), the LCDZ separates the 2.68–2.67 Ga old alkalic volcanic–clastic sedimentary Timiskaming Group to the north, from the 2705 Ma mafic volcanic–turbidite sedimentary Larder Lake Group to the south (Jensen 1985, Jackson & Fyon 1991). Recent seismic reflection surveys in the region indicate that the LCDZ dips steeply southward to a depth of at least 15 km (Jackson *et al.* 1990). At the surface, the LCDZ is a zone, up to 1 km wide, of intense ductile fabric development and alteration. Three separable phases of ductile fabric development have been identified within the LCDZ and on either sides (Toogood & Hodgson 1986, Hodgson & Hamilton 1989, Cruden 1991). The earliest phase, $D_1$, is that of interest in the present discussion; it is responsible for the bulk of the deformation in the LCDZ, and for the most significant aspects of the fabric and structures observed in outcrops (Wilkinson & Cruden 1992). Strain and related metasomatic alteration associated with $D_1$ show a markedly heterogeneous distribution. In the Timiskaming Group, north of the LCDZ, it produced E–W-trending, upright to N-verging folds, and local fault repetition of strata. To the south, in the Larder Lake Group metasediments, $D_1$ formed tight E–W-trending folds. Approaching the LCDZ, folds tighten and a penetrative bedding parallel cleavage is developed. Within the zone itself, $D_1$ is defined by a strong, flattening shape foliation or chloritic schistosity, a steeply but variably plunging stretching lineation (Fig. 3) and by strong carbonate ± chlorite ± talc alteration. In NW–SE- and NE–SW-trending segments of the zone, shear-sense indicators on horizontal planes suggest dextral and sinistral transcurrent motion respectively. Southeast of Dobie, for example, the LCDZ trends NW–SE (Fig. 2), the foliation dips steeply south, and the lineation, defined by strong clast elongation, plunges *ca* 60°E. Yet, dextral shear-sense indicators (rotated clasts in metaconglomerate) are well defined on horizontal erosional sections (Fig. 4a), but no indicators are observed on planes perpendicular to the foliation and parallel to the lineation (Fig. 4b). East–west-trending sections of the LCDZ record only N–S shortening and vertical extension (i.e. coaxial strains). Wilkinson & Cruden (1992) interpret these relationships to indicate that $D_1$ in the LCDZ resulted from N–S-shortening across a subvertical zone, producing flattening and vertical extrusion in

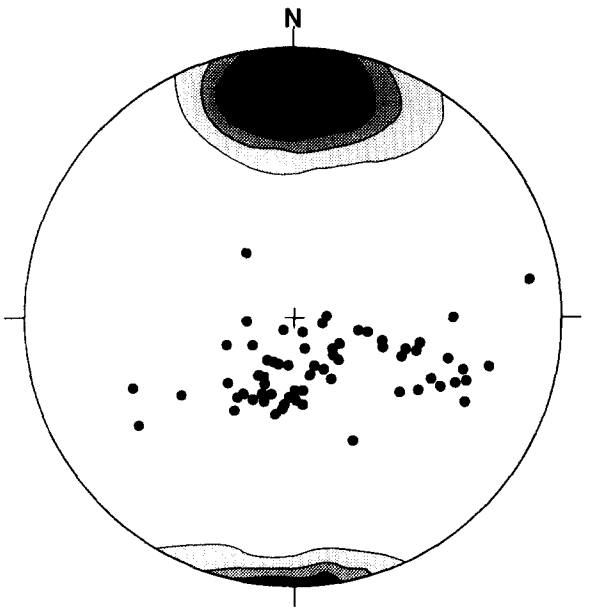


Fig. 3. Equal-area, lower-hemisphere projection of poles to $D_1$ foliation (143 poles, Kamb contoured, contour interval 6 $\sigma$) and $D_1$ stretching lineations (filled dots, 68 measurements) from within the area of the LCDZ shown in Fig. 2.

E–W-trending sections, and transpression in NE- and NW-trending segments. In the Val d'Or area, 180 km east of Kirkland Lake, where the LCDZ trends E to ESE, Robert (1989) similarly interprets steep stretching lineations, obliquity of foliations to the zone, and shear sense indicators visible on horizontal planes, as being the result of $D_1$ dextral transpression.

*The 'Mylonite Zone', SW Sweden*

The Mid-Proterozoic Sveconorwegian orogenic province of south-west Sweden and southern Norway (Fig. 5a) is divided into several sub-provinces by a network of roughly N–S-trending, predominantly W-dipping shear zones. Most of these shear zones, exposed between the west coast to the Sveconorwegian Front (Fig. 5a), are characterized by the presence of proto- to ultramylonites and well-developed stretching lineations. One important example is the 'Mylonite Zone' (MZ), which is well exposed on the east shore of a prominent peninsula (Värmlandsnäs) of Lake Vänern (Fig. 5a). Here, the MZ consists of a *ca* 5 km-wide zone of mylonitized granites and para- and orthogneisses. Mylonitic foliations dip uniformly to the west, with an average orientation of 178°/46°W, parallel to the inferred margins of the zone (Fig. 5b) (Stephens *et al.* 1993). Strong mineral stretching lineations show much greater variability (Fig. 5b), swinging gradually from west, almost down-dip, plunges in the eastern part (i.e. the footwall), to oblique north-west plunges in the centre, to shallow, northerly-trending, strike parallel orientations adjacent to the western boundary (hangingwall). Unlike the LCDZ, shear-sense indicators (winged porphyroclasts, *C–S* fabrics, mica fish, asymmetric extensional shear bands) are best observed on *XZ* sections of the fabric ellipsoid, as would be expected in progressive simple shear zones. Unlike simple shear zones, however, they track the swing in lineation orientation (Fig. 5b) and indicate reverse, dip-slip shear close to the footwall, oblique slip in the centre, and sinistral transcurrent shear adjacent to the hangingwall (Stephens *et al.* 1991). A sinistral transpressive tectonic regime has been inferred for this shear zone (Stephens *et al.* 1993).

Park *et al.* (1991) report a similar change of lineation orientation across the MZ approximately 90 km to the south, around Lake Mjörn. These authors interpret the lineation pattern as due to an early SE-directed thrusting (i.e. oblique-left-slip shear) followed by a later E-directed thrusting event (i.e. dip-slip shear). However, on the basis of the similar mineral parageneses associated with all foliations and lineations and of the absence of overprinting relationships, Stephens *et al.* (1993) argue that there is no evidence for two separate deformation events associated with the mylonitization in the MZ at Vämlandsnäs.

As summarized above, the LCDZ and the MZ show fabric and kinematic patterns which are inconsistent with those predicted by models of progressive simple shear zones. There is evidence that the deformation associated with both zones occurred within oblique convergent tectonic regimes (i.e. transpression). Sanderson & Marchini's (1984) SMTZ model does predict: (1) non-plane strain; and (2) the local occurrence of steep stretching lineations with transcurrent shear-sense indicators as observed in the LCDZ. But, because of its inherent homogeneity, it cannot account for other complexities of these zones. We show below that a slightly more realistic model of transpression can account for the following additional characteristics: (3) evidence for coaxial strains in addition to non-coaxial strains; (4) systematic variations in lineation orientation across the zone; and (5) presence of both transcurrent and dip-slip shear.

## THEORY

In the present work, we develop a dynamic model of the stress and strain distribution in a linear viscous material confined within a vertical transpression zone. We only explore the instantaneous, infinitesimal solution. That solution could, in principle, be iterated to model large accumulated strains explicitly (e.g. McKenzie 1979, Schmeling *et al.* 1988). Considering the fundamental oversimplifications inherent to many models, including ours (e.g. linear viscous behaviour, preset zone boundaries, constant motion parameters), we believe that qualitative but judicious extrapolation from the instantaneous to the finite strain patterns, when required, is sufficient to show their important features

A major advantage of linear viscosity and infinitesimal strain, as mentioned earlier, is our consequent ability to use the principle of superposition of two rheological solutions.

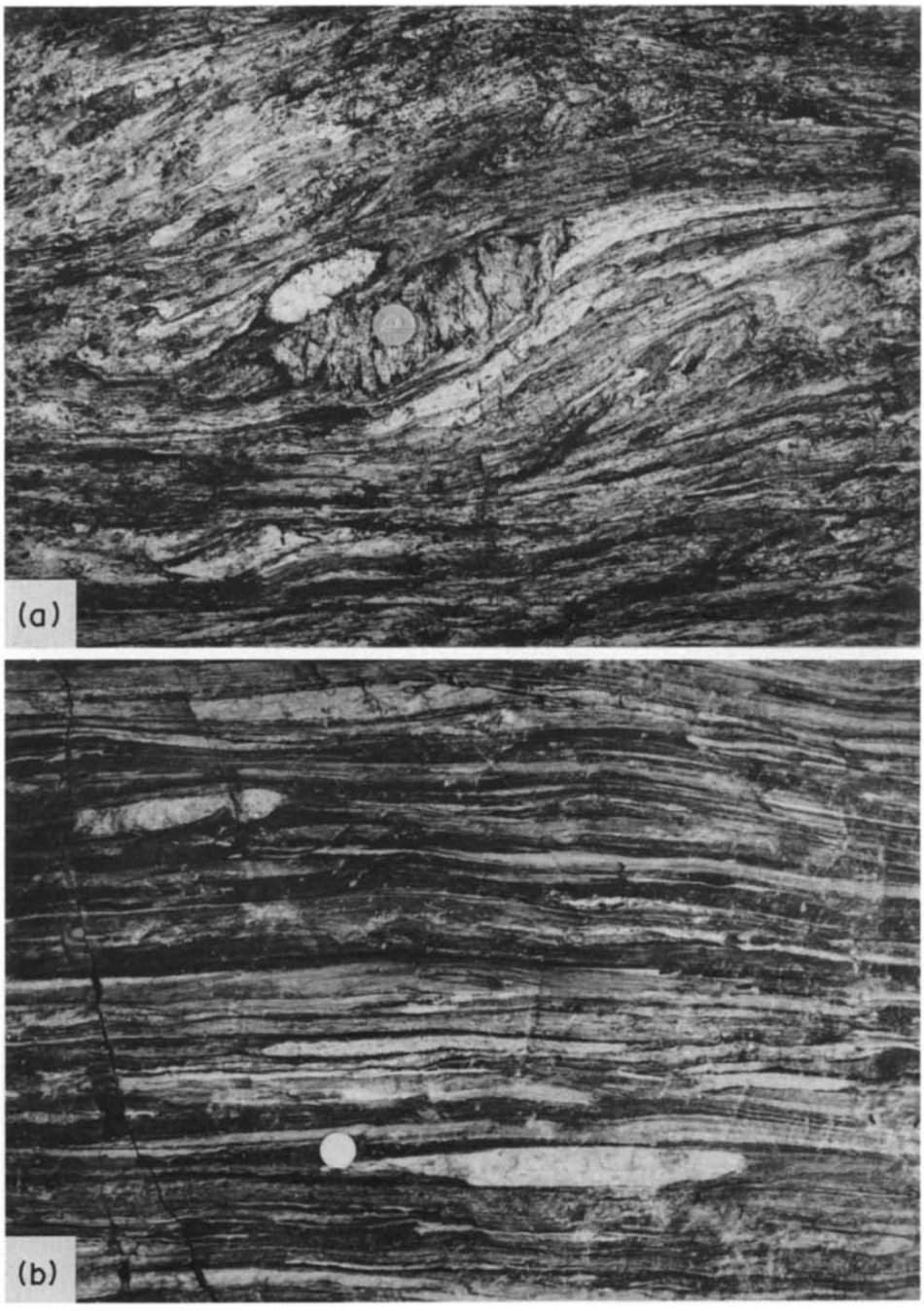


Fig. 4. Photographs of fabric relationships in deformed metaconglomerates in the Dobie area of the LCDZ (arrowed in Fig. 2). (a) Horizontal erosional surface showing large quartz–feldspar porphyry clast with the long axis inclined to the trace of $D_1$ foliation and 'tails' of strongly flattened bedding which curve into the foliation away from the clast, indicating a dextral sense of shear. Coin diameter = 2.1 cm. (b)Outcrop surface *ca* 15 m from (a), subparallel to the $D_1$ stretching lineation and perpendicular to the $D_1$ foliation. Note marked elongation of clasts and the absence of shear-sense indicators, which are present on horizontal sections 2 m along strike from location of this photograph. Coin diameter = 2.4 cm.

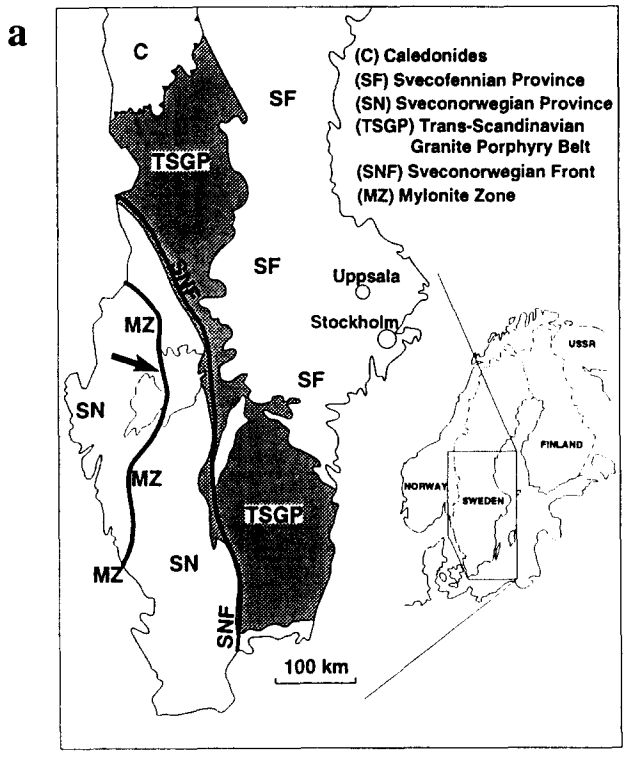


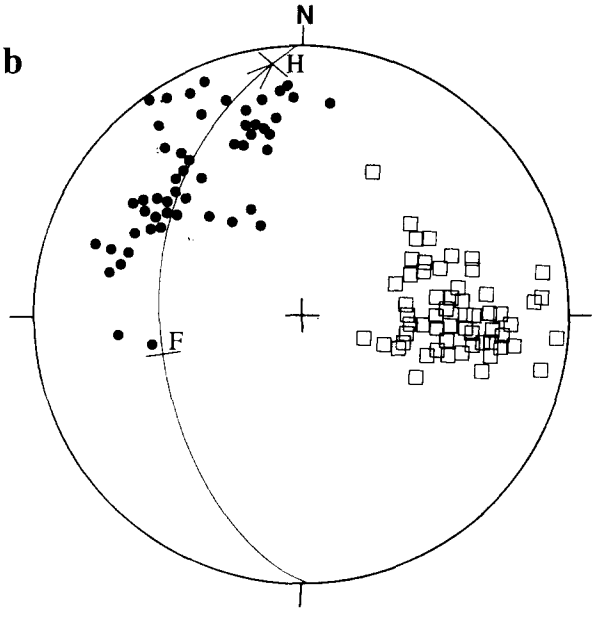


Fig. 5. (a) Map of southern Sweden showing the trace of the Mylonite Zone (MZ) in the Sveconorwegian province (SN). Arrow points to exposure of the MZ on the east shore of the Värmlandsnäs peninsula, Lake Vänern. (b) Equal-area, lower-hemisphere projection of structural data collected by M. B. Stephens and C.-H. Wahlgren (Geological Survey of Sweden) from the MZ at Värmlandsnäs. Open squares: poles to mylonitic foliation; filled circles: stretching lineations; great circle: average orientation of the foliation in the zone. Lineation swings in direction of arrow from down-dip in rocks close to the footwall (F) to almost strike-parallel adjacent to the hangingwall (H). Kinematic indicators in the zone track the lineation and give reverse dip-slip shear close to the footwall and sinistral transcurrent shear adjacent to the hangingwall, as predicted by the model of oblique transpression summarized in Fig. 13.

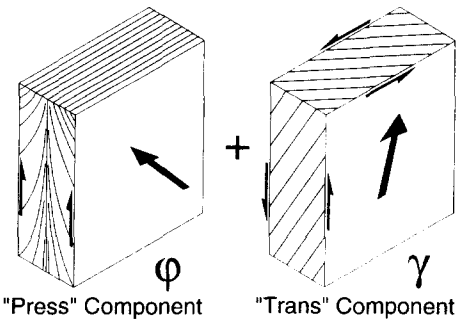


Fig. 6. Principle of superposition of two linear viscous flows. Large arrows: movement vectors of the zone boundaries; half arrows: horizontal and vertical components of motion at the zone boundaries.

*Superposition of 'press' and 'trans'*

We can model transpression as the superposition of the solutions to two boundary-value problems (Fig. 6): that of the extrusion of the material, related to the 'press' component of the wall motion, and that of shearing parallel to the wall of the zone, related to the 'trans' component of the motion. Figure 7 defines the parameters and the co-ordinate system used. The zone is assumed to be vertical, with a half-width $h$, the $x$-axis is horizontal and parallel to the zone, the $y$-axis is horizontal and perpendicular to the zone, and the $z$-axis is vertical, with $z$ increasing upward, i.e. in the escape direction. The angle which the shear direction makes with the horizontal, is $\beta$, which thus describes the obliquity of the transpressive motion.

The extrusion of a viscous liquid between two rigid plates approaching each other is a classic boundary-value problem. Jaeger (1962, pp. 140 & ff.) presents a solution to it as example of the use of stream functions, and gives the result as a velocity field. Appendix A derives the corresponding velocity gradient tensor.

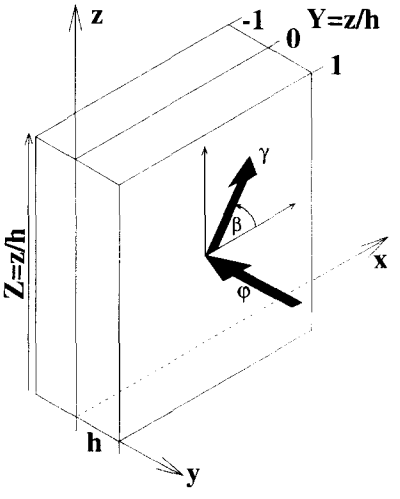


Fig. 7. Co-ordinate system used in the transpression models and definitions of normalized height ($Z$) and normalized zone width ($Y$) and orientation of the progressive simple shear direction ($\beta$).

To Jaeger's (1962) rate of approach of each wall toward the mid plane, $V_0$, we substitute a strain rate parameter $\varphi = V_0/h$; $\varphi$ can be viewed as an average rate of flattening strain across the zone, comparable to Sanderson & Marchini's (1984) parameter $\alpha$. Similarly, the shear component of the wall displacements is described by a rate of simple shear, $\gamma$. It is important to recognize that $\phi$ and $\gamma$, used to describe the boundary conditions for the zone, are only bulk strain rate parameters. Unlike in the SMTZ, the strain here is heterogeneous, and thus $\phi$ and $\gamma$ do not describe the actual flattening and shearing rates at any particular point within the zone. A convenient parameter is: $f = \phi/\gamma$, which we also refer to as the 'press'/'trans' ratio. For convenience, even though the zone is assumed vertical, we shall refer to the side which is moving up with respect to the other as the hanging-wall, and to the other side as the footwall.

The total velocity gradient tensor resulting from the superposition of the two deformations is given by equation (1):

$$\begin{bmatrix} \frac{\partial u}{\partial x} & \frac{\partial u}{\partial y} & \frac{\partial u}{\partial z} \\ \frac{\partial v}{\partial x} & \frac{\partial v}{\partial y} & \frac{\partial v}{\partial z} \\ \frac{\partial w}{\partial x} & \frac{\partial w}{\partial y} & \frac{\partial w}{\partial z} \end{bmatrix} = \begin{bmatrix} 0 & \gamma\cos\beta & 0 \\ 0 & -\frac{3}{2}\varphi(1-Y^2) & 0 \\ 0 & \gamma\sin\beta - 3\varphi YZ & +\frac{3}{2}(1-Y^2) \end{bmatrix}, \quad (1)$$

where

$u, v, w$ are the components of velocity;

$Y = y/h$ is the normalized distance from the central symmetry plane of the transpression zone, normalized to the half-thickness, $h$, of the zone; and

$Z = z/h$ is the normalized height above the base of the transpression zone.

This velocity gradient tensor can be separated into its symmetric and antisymmetric part (e.g. see Means *et al.* 1980), thus giving the symmetric *strain rate tensor*, $\varepsilon$, the antisymmetric *rotation rate tensor*, $\omega$, and the corresponding *external vorticity vector*, $\Omega$:

$$\varepsilon = \frac{\gamma}{2}\begin{bmatrix} 0 & \cos\beta & 0 \\ \cos\beta & -3f(1-Y^2) & \sin\beta - 3fYZ \\ 0 & \sin\beta - 3fYZ & 3f(1-Y^2) \end{bmatrix}$$

$$= \begin{bmatrix} 0 & \varepsilon_{xy} & 0 \\ \varepsilon_{xy} & -\varepsilon_{zz} & \varepsilon_{yz} \\ 0 & \varepsilon_{yz} & +\varepsilon_{zz} \end{bmatrix} \quad (2)$$

$$\omega = \frac{\gamma}{2}\begin{bmatrix} 0 & \cos\beta & 0 \\ -\cos\beta & 0 & -\sin\beta - 3fYZ \\ 0 & \sin\beta - 3fYZ & 0 \end{bmatrix}$$

$$= \begin{bmatrix} 0 & \varepsilon_{xy} & 0 \\ -\varepsilon_{xy} & 0 & -\varepsilon_{yz} \\ 0 & \varepsilon_{yz} & 0 \end{bmatrix} \quad (3a)$$

$$\Omega = \begin{bmatrix} \frac{\partial w}{\partial y} - \frac{\partial v}{\partial z} \\ \frac{\partial u}{\partial z} - \frac{\partial w}{\partial x} \\ \frac{\partial v}{\partial x} - \frac{\partial u}{\partial y} \end{bmatrix} = 2\begin{bmatrix} \varepsilon_{yz} \\ 0 \\ -\varepsilon_{xy} \end{bmatrix}. \quad (3b)$$

Model results are thus obtained by calculating the strain rate components along a vertical section, $yz$, normal to the zone, for set values of $f$ and of the obliquity, $\beta$. The parameters which have been calculated as a function of position in the zone are discussed below.

*Strain rate ellipsoid parameters*

At each point we first compute the principal directions and the principal components of strain rate, $s_1$, $s_2$ and $s_3$, which can then be used to calculate strain ellipsoid shape and strain intensity parameters, $K$ and $D$.

K-*value*. For strain rates, as well as for infinitesimal strains, both Flinn's $k$-value and Ramsay's $K$-value (e.g. see Ramsay & Huber 1983, p. 200) reduce to:

$$K = k = \frac{s_1 - s_2}{s_2 - s_3}. \quad (4)$$

As for finite strain, there is no 'lineation' when $K = 0$, and no 'foliation' when $K = \infty$. In practice, a lineation may not have any petrographically visible expression when $K$ is below a certain critical value, e.g. 0.3 or 0.4.

*Strain rate intensity*, D. Similarly, intensity parameters $d$ and $D$ (Ramsay & Huber 1983, p. 202) both reduce, but for the same factor of $\sqrt{2}$, to:

$$D = d = \sqrt{2[(s_1 - s_2)^2 + (s_2 - s_3)^2]}. \quad (5)$$

The factor $\sqrt{2}$ is introduced here to normalize the results to the strain rate intensity for a simple shear zone (i.e. for $f = 0$): in a progressive simple shear zone which would shear homogeneously at the same bulk rate $\gamma$, $D$, as defined in equation (5), would be 1 everywhere.

*'Foliation' and 'lineation'*

We refer to the maximum, intermediate and minimum principal directions of the strain rate ellipsoid as the $A$, $B$ and $C$ direction, respectively, corresponding to

the principal strain rate components $s_1$, $s_2$ and $s_3$. Thus the $A$ direction is that of the maximum extension rate, $s_1$; we also refer to it as the 'lineation'. The $A$ and $B$ directions define a plane of instantaneous flattening, which we also call 'foliation'.

In nature, lineations and foliations are commonly interpreted in terms of the principal directions of *total accumulated strain*. Since the strain rate of equation (2) is in effect equal to an infinitesimal strain increment, the model 'lineations' and 'foliations', based on principal directions of the *strain rate tensor*, would be correct predictors only for small strains. Indeed, since the vorticity (equation 3) is not zero, the principal strain directions of the finite strain ellipsoid can, for large strains, differ significantly from those of the strain rate tensor. The use of 'lineation' and 'foliation' can therefore 'invite over-interpretation of the results', as remarked by F.W. Vollmer (personal communication 1993). Nevertheless, 'lineation' and 'foliation', accompanied by the present warning, are useful terms for several reasons.

(i) They are much easier to read and grasp than their terminologically rigorous equivalents.

(ii) For small accumulated strains, lineations and foliations would be close to the 'lineations' and 'foliations' of the incremental models.

(iii) The natural prototypes to which the model zones are compared are known by their distributions of foliations and lineations. It is indeed our task below, and the very objective of the present work, to try and predict the lineations and foliations of a finite strain model from the 'lineations' and 'foliations' of our incremental model.

### *Vorticity*

*External vs internal vorticity.* The vorticity $\omega$ calculated from equation (3) is the external vorticity, describing an average rotation of material lines with respect to a fixed, external co-ordinate system. External vorticity can be used to predict how principal strain directions for small deformations will be rotated, with respect to that coordinate system, after large accumulated deformation. But the vorticity which is expressed in the fabric of the rock, that which is estimated with *shear-sense indicators* (designated here also as *vorticity indicators*), is the internal vorticity (Means *et al.* 1980). The internal vorticity tracks the rotation of lines within the rock with respect to the principal directions of strain rate.

In a progressive simple shear zone, or in the SMTZ model, the principal strain rate directions around a material particle do not rotate with respect to the external co-ordinates as the particle moves; the internal vorticity is therefore identical to the external vorticity. But in the present model of transpression, a particle does in fact change its relative position $(Y, Z)$ within the shear zone, and therefore the principal directions of its strain rate rotate with respect to the external reference frame. Means *et al.* (1980) proposed to call *spin* the rotation of the principal directions of strain as a particle moves. Appendix B gives the theory and the method which have been used to calculate the spin tensor, $\rho$, at a number of grid points. The magnitude of the spin vector, $|P|$, is found to be always smaller than that of the external vorticity, $|\Omega|$. However, the former may reach 25% of the latter at high elevations and for high values of the 'press'/'trans' ratio $f$ (Appendix B). The spin is therefore not always everywhere negligible. Nevertheless, the spin was neglected in the calculation of a sectional vorticity number below because such neglect makes the computations and the presentation of the results easier.

*Kinematic vorticity number.* Means *et al.* (1980) noted that a parameter to quantify the development of shear-sense indicators should normalize the internal vorticity to the strain rate intensity. A convenient parameter to that effect is the three-dimensional *kinematical vorticity number*, defined by Truesdell (1953) as

$$W_k = \frac{|\Omega|}{\sqrt{2(s_1^2 + s_2^2 + s_3^2)}}. \quad (6)$$

In the usual case of plane isovolumetric strain, in which $s_2 = 0$ and $s_1 + s_3 = 0$, equation (6) reduces to:

$$W_k = \frac{|\Omega|}{s_1 - s_3}. \quad (7)$$

A vorticity vector can be viewed as a rotation axis; the geologist should expect to see the vorticity indicator best displayed on a face normal to the internal vorticity vector, at least in an initially isotropic rock. We propose to call the plane normal to the vorticity vector the *vorticity profile plane*. For the geologist examining the vorticity profile plane for shear-sense indicators, a three-dimensional kinematic vorticity number more appropriate than Truesdell's $W_k$, is a *sectional kinematic vorticity number*, $W_k^s$, in which the vorticity is normalized to the sectional strain in the vorticity profile plane:

$$W_k^s = \frac{|\Omega|}{s_1^s - s_2^s}, \quad (8)$$

where $s_1^s$ and $s_2^s$ are the principal components of sectional strain. $W_k^s$ reduces of course to $W_k$ in the case of plane strain. For the strain given in equations (2) and (3), a laborious but otherwise straightforward derivation yields:

$$W_k^s = \sqrt{\frac{(\varepsilon_{xy}^2 + \varepsilon_{yz}^2)^3}{[\varepsilon_{zz}(\varepsilon_{xy}^2 + \varepsilon_{yz}^2)]^2 + 4(\varepsilon_{xy}^2 + \varepsilon_{yz}^2)^3}}. \quad (9)$$

As discussed in the preceding section and in Appendix B, the sectional vorticity number calculated with this formula and represented in Fig. 10 is not quite accurate when $f$ and $Z$ are high and $Y$ is between 0.15 and 0.3.

### *Implementation*

All calculations were carried out with TRPR.M, a program written in the MATLAB language. MATLAB is a high-level interpreter/compiler language specialized in efficient numerical matrix operations. The diagonalization of the strain in equation (2) was thus done

numerically from the values of the strain components calculated at grid points on a $YZ$ section.

## RESULTS

Results are presented for two cases of 'transcurrent' transpression ($\beta = 0°, f = 0.1$ and $f = 1$) and one case of oblique transpression ($\beta = 75°$, $f = 1.5$). Since for a given elevation, $Z$, and a given distance, $Y$, from the mid-plane, the strain is independent of $X$, we only need to show the results on a $YZ$ profile in each case.

It is necessary to recall that the 'lineations' and 'foliations' presented are only predicted by the $A$ and the $C$ directions of the instantaneous strain rate ellipsoid. One of the results discussed below is that the sectional vorticity number, $W_k^s$, is everywhere close to 1, i.e. close to its value for progressive simple shear. We can therefore anticipate that, with time, accumulated deformation will bring both foliations and lineations into closer parallelism with the zone boundaries. This uniformly high value of $W_k^s$ also suggests that vorticity indicators might be observed everywhere in the zone.

Another result is that the $K$-value can vary from 1 to 0 within a single zone. The 'lineation' may therefore not be expressed petrographically everywhere; we may assume for example that no lineation would be visible when $K < 0.3$ or 0.4. We have not investigated in what way large accumulated strains would affect the value of $K$ as calculated from the instantaneous strain.

### *'Transcurrent' transpression*

Figures 8–11 summarize results for the two cases ($f = 0.1$ and $f = 1$) of dextral, transcurrent transpression ($\beta = 0°$).

*Fabric pattern.* All transcurrent models have symmetric fabric patterns: any one vertical line in the midplane is a two-fold axis of symmetry. In profiles, 'foliations' show an inward increase in apparent dip, and are vertical in the centre of the zone (Figs. 8a & b and 9b). In horizontal sections (Figs. 8a and 9a), the 'foliation' changes orientation across the zone: from striking at a low angle to the zone at its boundaries, it swings to 45° to the zone boundaries near the midplane. This appears to be in contrast with a transcurrent simple shear zone (Ramsay & Graham 1970), in which the foliation pattern swings from 45° to the zone near the walls to a lesser angle in the centre. These two patterns are not strictly comparable, however, since that shown here is for an incremental strain, whereas the pattern commonly associated with a Ramsay and Graham shear zone is for accumulated strains; the pattern of 'foliation' trajectories in a vertical Ramsay and Graham shear zone would in fact be a set of straight lines at 45° to the zone boundaries. The difference between the strike of the 'foliation' and that of the zone boundaries, which is greatest in the centre, decreases with higher 'press' components.

Variations in the plunge of the 'lineation' across a zone are strongly dependent on the magnitude of the 'press' component. It can be shown that for, $f < 1/(3\sqrt{2}) = 0.236$, the 'lineation' is horizontal along the midplane ($Y = 0$) regardless of the elevation $Z$, whereas it is vertical, again regardless of the elevation $Z$, when $f > 0.236$. For $f = 0.236$, $K = 0$ on the midplane and there is no 'lineation'. In the SMTZ model, the 'press'/'trans' ratio for the similar transition is $f = 1/(2\sqrt{2}) = 0.354$. The difference between the SMTZ and the present model stems from the fact that the 'press' component of the deformation is concentrated in the centre of the zone in the present model, whereas it is uniformly distributed in the SMTZ model (see the coefficient $\frac{3}{2}$ in equation 1).

*Fabric parameters.* The deformation rate intensity, $D$, is, we recall, normalized to the value it would have in a non-transpressive zone shearing at the same rate $\gamma$ (equation 5). For both cases illustrated, $D$ is greater than, but close to, 1 near the centre and base of the zone (Figs. 8c and 9c). From there, $D$ always increases upwards in the zone, and, in any one level, always increases toward the margins. This is a direct expression of the extrusion process. For a strong 'press' component ($f = 1$), the extrusion process dominates and $D \gg 1$ throughout most of the zone (Fig. 9c): strain rate intensities are much greater than those expected in a simple shear zone.

As stated earlier, $K$-values are an important measure of the predicted petrographic expression of the fabric. For a low press component ($f = 0.1$, Fig. 8d) an upwards narrowing region with $K < 0.4$ occurs in the centre of the zone. Hence, the parts of the zone characterized by a horizontal A direction are expected to show little or no lineation. In all cases, plane strain conditions, i.e. $K \sim 1$, are found near the zone margins, over a width which increases with elevation and with $f$. With the higher $f$ value ($f = 1$, Fig. 9d) $K \gg 0.4$ everywhere except at the bottom of the zone, and is close to 1 over a wide part of the outer portions of the zone at high levels. Like the strain intensity, these patterns of $K$ values are a direct consequence of the extrusion process.

*Vorticity.* We recall that the external vorticity presented here differs slightly from the internal vorticity since, as explained and justified in Appendix B, we have neglected a spin component. The external vorticity vector is always parallel to the $XZ$ plane (see equation 3). Figures 8(e) and 9(e) show the plunge of the vorticity vector, with its sign chosen such that clockwise (or dextral) vorticity on the vertical profile is considered positive. Variations in the sectional kinematic vorticity number, $W_k^s$, are shown in Fig. 10. For $f = 0.1$, $W_k^s$ decreases from a value of 1 at the zone margins to a minimum of 0.9884 close to the centre at normalized height $Z = 8$. With $f = 1$, $W_k$ reaches minimum values of 0.5488 in two narrow regions adjacent to the zone centre at normalized height $Z = 8$. We therefore expect the development of vorticity indicators everywhere in the

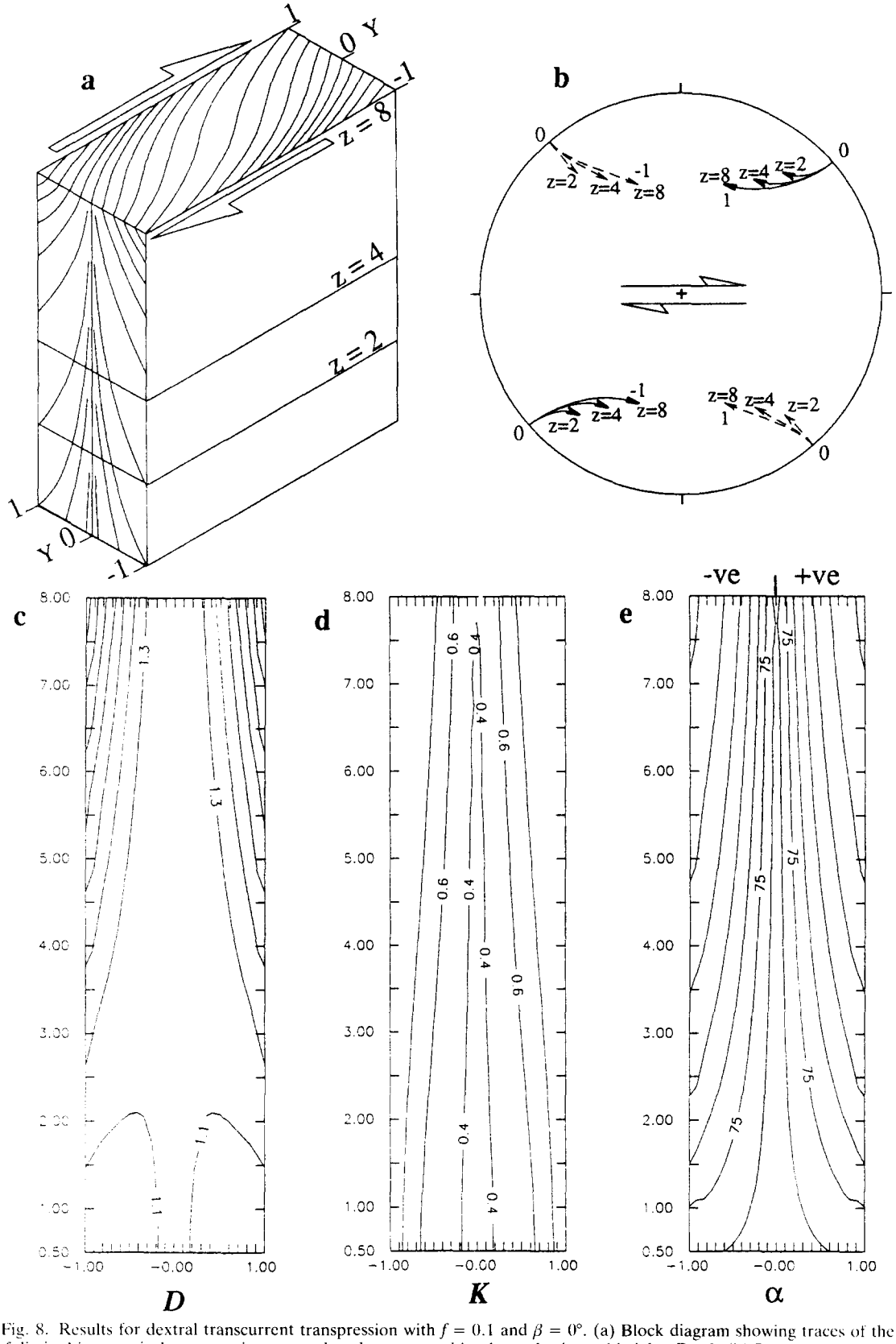


Fig. 8. Results for dextral transcurrent transpression with $f = 0.1$ and $\beta = 0°$. (a) Block diagram showing traces of the 'foliation' in a vertical cross-section, normal to the zone, and in plan at horizontal height, $Z = 8$. (b) Equal-area, lower-hemisphere projection of the change in 'lineation' directions (solid lines) and poles to 'foliation' (dotted lines) across the zone at normalized heights, $Z = 2$,4 and 8. (c) Contours of strain intensity ($D$) values in a vertical cross-section normal to the zone. Contour interval = 0.2. (d) $K$-value contours (interval = 0.2). (e) Contours of the plunge angle of vorticity vectors (interval = 10°, values decrease towards outer edge of zone). See text for definition of positive and negative vorticity.

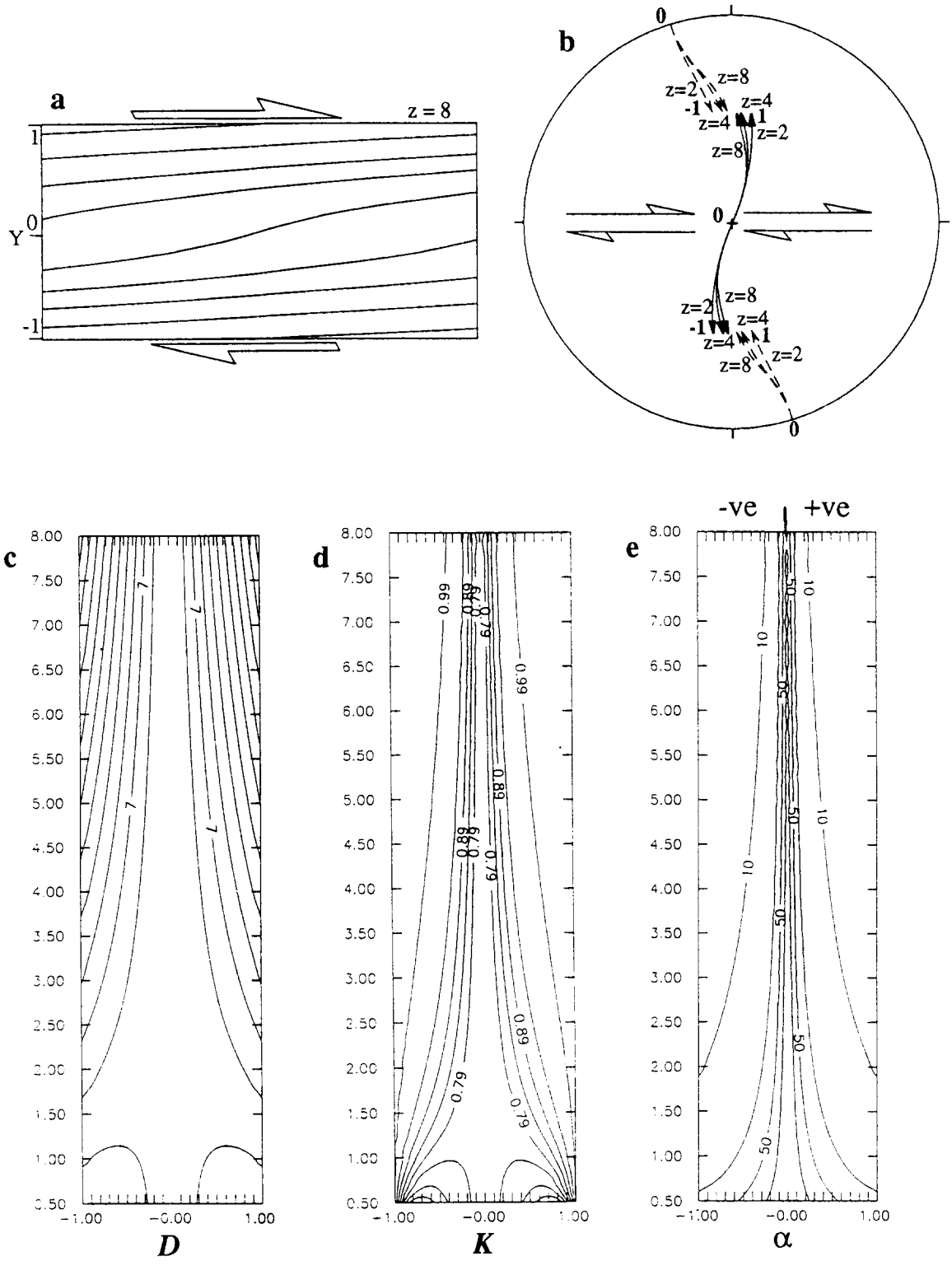


Fig. 9. Results for dextral transcurrent transpression with $f = 1.0$ and $\beta = 0°$. (a) Trace of the 'foliation' at $Z = 8$ level. (b) 'Lineation' and 'foliation' orientations, as in Fig. 8. (c) $D$-values, as in Fig. 8. Contour interval = 2, values increase outwards and upwards. (d) $K$-values, as in Fig. 8. Contour interval = 0.05. (e) vorticity vector plunges, as in Fig. 8. Contour interval = 20°.

zone, regardless of the magnitude of the press component.

For both $f = 0.1$ and $f = 1$, the vorticity vector is vertical in the midplane and decreases to shallow plunges near the margin. Or, expressed in terms of the orientation of the rock faces on which the geologist should look for indicators, the vorticity profile plane is horizontal in the centre and steepens up toward to margins of the zones. Comparing Figs. 8(e) and 9(e), we see that a higher 'press' component leads to a narrower zone with steep plunges of the vorticity vector and to shallower plunges over more of the zone. For example, at normalized level $Z = 6$, the half-width of the region within which the plunge of the vorticity vector is steeper than 45° is given by $1/(18f)$, and is therefore $0.555\,h$ for $f = 0.1$, $0.222\,h$ for $f = 0.25$ and $0.055\,h$ for $f = 1$.

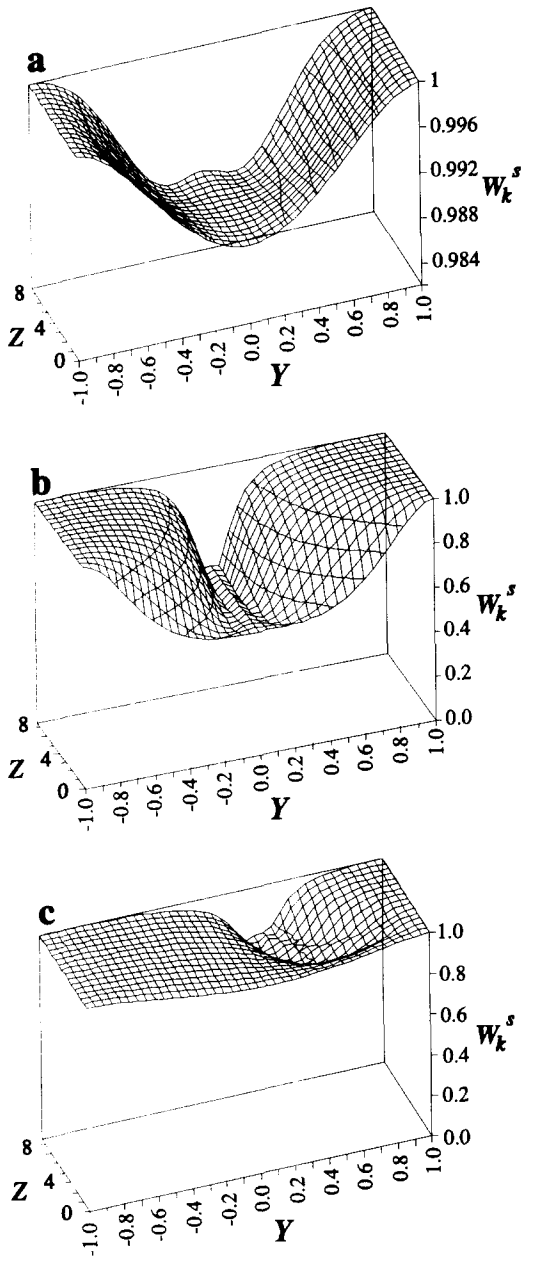


Fig. 10. Mesh diagrams showing the variation of $W_k^s$ in the vertical ($Z$) and horizontal ($Y$) directions in the zone. (a) Transcurrent transpression with $f = 0.1$ and $\beta = 0°$. (b) Transcurrent transpression with $f = 1.0$ and $\beta = 0°$. (c) Oblique transpression with $f = 0.15$ and $\beta = 75°$. 'Hanging-wall' is on $Y = 1$ side.

Clearly, for $f = 1$, vorticity is dominated by the extrusion process, except very close to the midplane and near the base of the zone.

*Zone kinematics.* Figure 11 summarizes the fabric and vorticity pattern predicted for a transcurrent transpression zone at a normalized height $Z = 8$ and for the two cases $f = 0.1$ and $f = 1$. In both cases all levels show similar patterns, except for the very lowest ($Z < 1.5$).

For a 'press'/'trans' ratio $f = 0.1$ (Fig. 11a) the rocks are predicted to exhibit a nearly monoclinic fabric throughout the zone: that is the vorticity indicator is always close to orthogonal to the stretching lineation, or, stated differently, the vorticity profile plane always contains the lineation. However, an interesting pattern is still predicted. Near the midplane, horizontal lineations and vertical vorticity indicators are similar to those in a simple shear zone or those in a SMTZ with $f < 0.354$. But, as one traverses away from the midplane, the lineation and the vorticity vector both rotate to yield an oblique, almost dip-slip, zone-side-up kinematic pattern near the margin.

For $f = 1$, and in fact, as noted earlier, for any $f > 0.236$, the vorticity is vertical and parallel to the 'lineation' in the centre of the zone. Strictly speaking, along the midplane, the fabric symmetry is monoclinic, but it is clearly not the usual symmetry expected in progressive simple shear: the two-fold axis is parallel to the 'lineation' rather than perpendicular to it. As one moves away from the midplane, the fabric becomes triclinic, and then becomes close to monoclinic again toward the margin. The width of the region within which the fabric symmetry effectively departs from the usual symmetry depends on the normalized level, $Z$, and on the ratio, $f$: that width decreases as both parameters increase. If we assume for example that the departure from the usual symmetry becomes petrographically detectable when the angle between the vorticity vector and the B direction exceeds 25°, this region decreases from $-0.27 < Y < +0.27$ at $Z = 2$, to $-0.07 < Y < +0.07$ at $Z = 8$.

The above transcurrent transpression models have duplicated a number of the features shown by the LCDZ and MZ: (1) strains with $K$-values which may vary from 0 to 1; (2) departure of the fabric symmetry from that expected in simple shear zones; (3) systematic variations of the lineation orientation; and (4) coexistence at the same exposure level, $Z$, of transcurrent, oblique and dip-shear. However, a major feature of these models is their symmetry. In particular, the two-fold symmetry of the models is reflected in the opposite signs of the vorticity across the midplane: a transcurrent ductile transpression zone should show opposite vorticities, related to the extrusion, on opposite walls of that zone. We are not aware of any report in the literature of a similarly symmetric geological prototype. It is the asymmetry found in natural transpression zones like the MZ that we want to model with oblique transpression.

*Oblique transpression*

Oblique transpression is, we recall, when $\beta \neq 0°$, i.e. when the shear direction is oblique, rather than parallel to the strike of the zone. A feature common to all cases of oblique transpression is that fabric and vorticity patterns across the zone are no longer symmetrical about a vertical axis through the centre. Furthermore they also show considerable depth ($Z$) dependence. Results for the case of sinistral oblique transpression with $\beta = 75°$ and $f = 0.15$ are presented in Figs. 10(c), 12 and 13. We have chosen to focus on this particular example because it demonstrates how an entirely asymmetric fabric and vorticity pattern can occur within a general transpression zone.

Figure 12 shows various parameters on vertical profiles perpendicular to the zone. The trace of the 'folia-

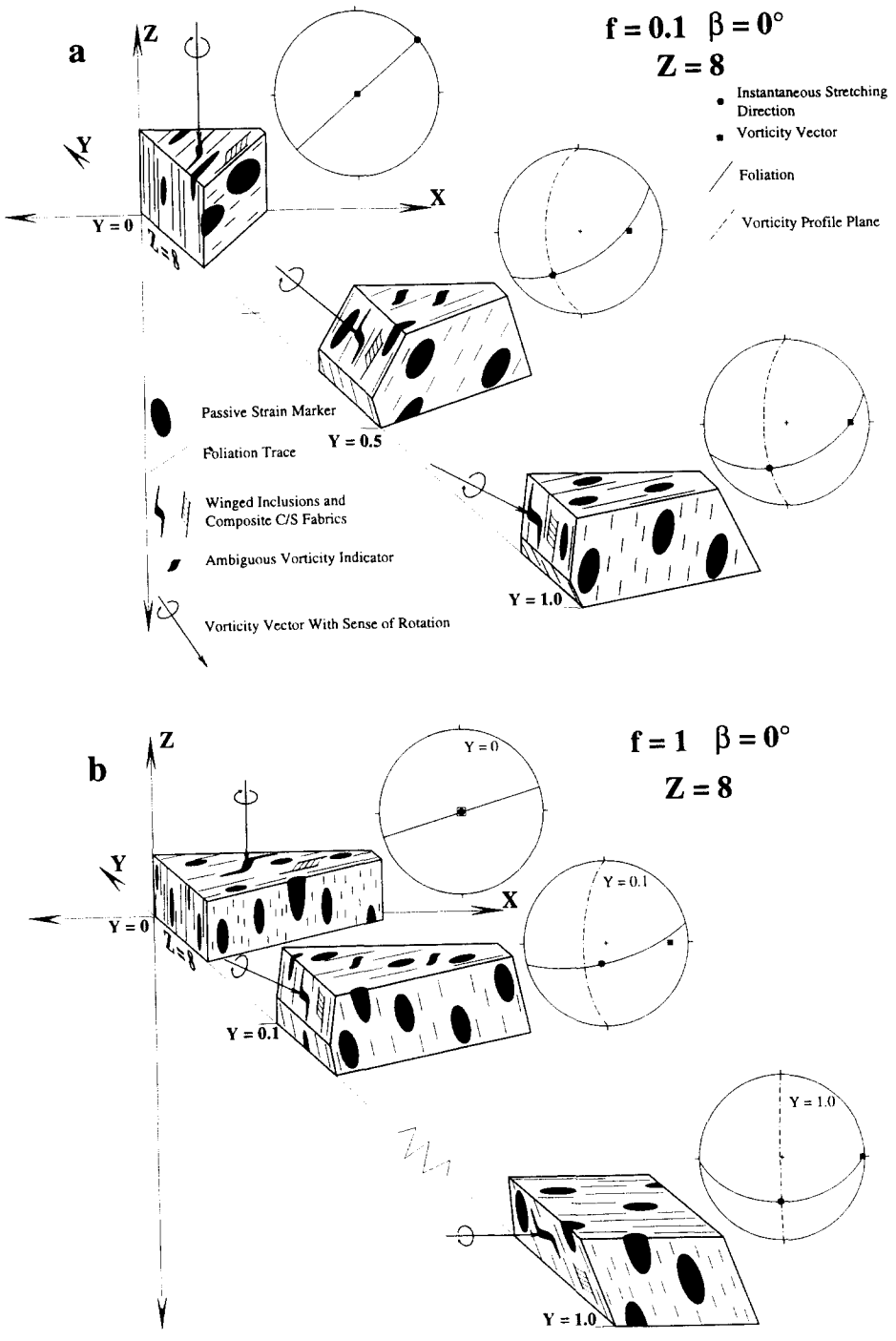


Fig. 11. Predicted fabric and kinematic patterns in the $Y = 0$–1 half and $Z = 8$ level of transcurrent dextral transpression zones with (a) $f = 0.1$ and (b) $f = 1.0$.

tion' in a vertical profile of the zone shows a distinctly asymmetric pattern (Fig. 12a). Below $Z = 2.25$ 'foliations' dip towards the footwall throughout the whole width of the zone. At higher levels, the dip direction does change along a horizontal traverse, and, as $Z$ increases, the point at which the 'foliation' is vertical migrates toward the centre of the zone. Deformation rate intensity values ($D$, Fig. 12b) are skewed, with the lowest values occurring in the lower parts of the zone on the hanging-wall side. Note that an area with $D < 1$ is found in the hanging-wall half of the zone. $K$-values (Fig. 12c) are lowest in the region centered about a point with co-ordinates $Y = 0.75$, $Z = 2.8$. A small elongate region with $K < 0.4$ (i.e. poorly expressed lineation) occurs between $Z \sim 2.3$ and $Z \sim 5$ near the hanging-wall. Exhibiting a pattern similar to the dip of the foliation, the vorticity (Fig. 12d) is negative (i.e. sinistral senses of shear) throughout the width of the zone for $Z < 2.2$. Above this level, extrusions becomes more important, and the vorticity shows a reversal similar to that in the transcurrent case, with the reversal point moving towards the centre as the level rises.

The sectional kinematic vorticity number, $W_k^s$, is close to 1 everywhere at the base of the zone, with a trough of

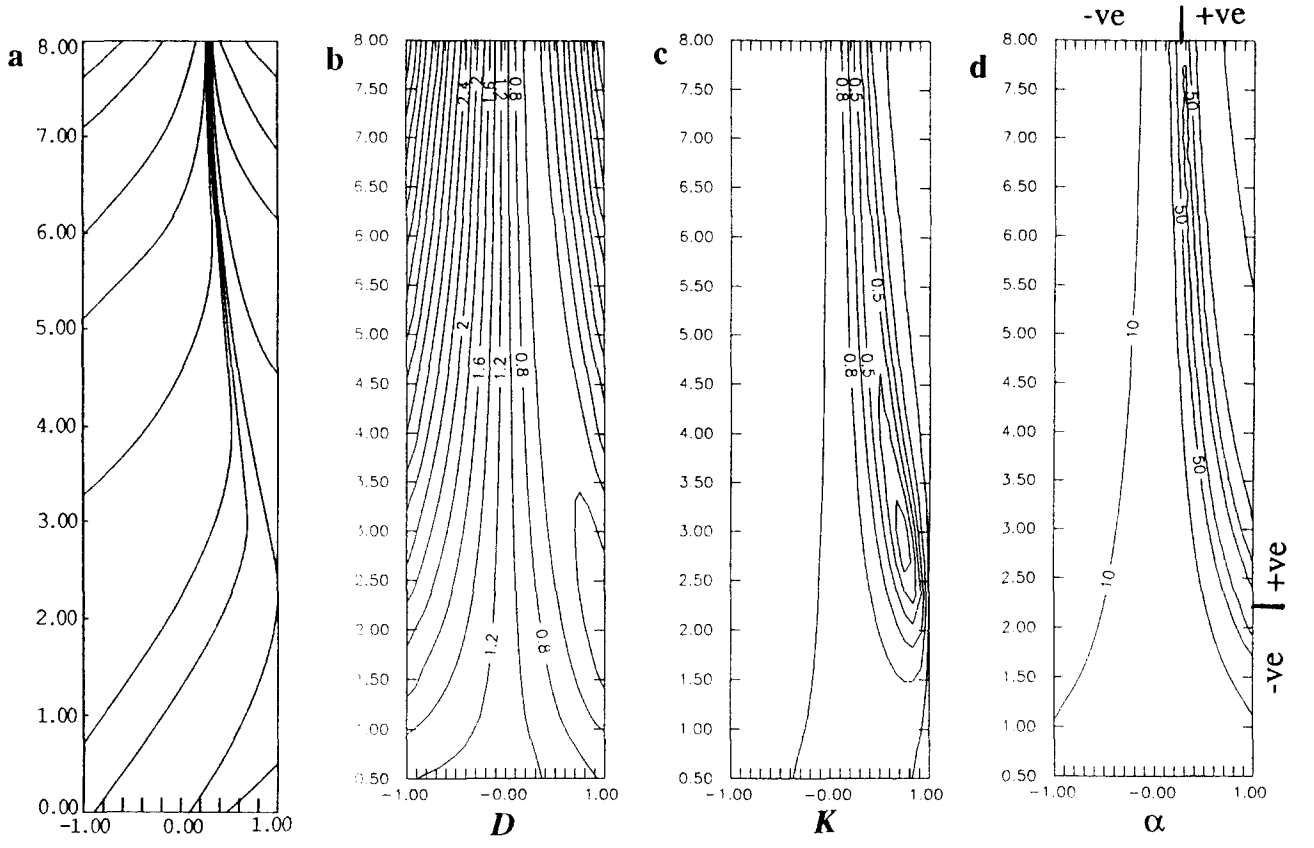


Fig. 12. Results, in vertical cross-section normal to zone, for sinistral oblique transpression model with $f = 0.15$ and $\beta = 75°$. 'Hangingwall' is on $Y = 1$ side. (a) 'Foliation' traces. (b) $D$-value contours (interval = 0.2). (c) $K$-value contours (interval = 0.15). (d) Contours of vorticity plunge (interval = 20°). See text for discussion of positive and negative vorticity.

lower values on the hanging-wall side (Fig. 10c). This trough migrates inwards towards the top of the zone where, at $Z = 8$, the lowest recorded value of $W_k^s = 0.7651$.

'Foliation' and 'lineation' trajectory maps for two horizontal levels of the model are shown in Fig. 13. Level $Z = 2$ is just below the level (see Fig. 12) where the fabric pattern changes from entirely asymmetric to skew symmetric. Here (Fig. 13a), the 'lineations' rake steeply at the footwall and rotate across the zone to the hanging-wall where they are parallel to the strike of the 'foliation' (Fig. 13a). Vorticity vectors indicate reverse, zone-side-up displacement at the footwall and sinistral transcurrent movement adjacent to the hanging-wall. At this level, the fabric symmetry is close to monoclinic throughout the zone. Both 'foliation' and 'lineations' make a high angle with the zone boundaries. But these correspond, we recall, to the principal direction of the initial incremental strain; after finite deformation, the external vorticity will cause a steepening of foliations and a decrease of the angles which foliations make with the margins. Likewise, lineations will also steepen at the footwall side because of the horizontal vorticity vector. However, the vorticity vector is vertical on the hanging-wall side, which will result in a rotation of the lineation towards the orientation of the margin, without causing a significant increase in plunge. The predicted fabric pattern, after a finite amount of deformation, is therefore very similar to that shown by the Mylonite Zone, in which the lineation was noted to vary gradually from down-dip near the footwall to strike-parallel near the hanging-wall (Fig. 5b).

At level $Z = 4$ (Fig. 13c), the fabric and vorticity pattern is similar to the $Z = 2$ case for $-1 < Y < +0.5$. However, both triclinic fabrics and a flip in 'foliation', 'lineation' and vorticity directions occur at $Y \sim 0.53$ (see also $Z = 4$ in Fig. 12). The overall pattern is therefore skew symmetric, with close to dip-slip kinematics related to extrusion prevalent throughout the zone except for a region near $Y = 0.5$ where the 'lineation' is vertical but the vorticity is also vertical (i.e. transcurrent sense of shear).

## DISCUSSION

### *Sizes and shapes of transpression zones*

*Scale and direction of transpression.* Transpression phenomena can occur at all scales, from microscopic to regional: e.g. a finer-grained matrix escaping between two phenocrysts or porphyroblasts; or a relatively incompetent unit or group of units squeezed from between two competent plutons. In either of these two cases, the 'escape' direction may not be vertical. But the original and still usual meaning of transpression is the regional one, with the escape direction understood to be

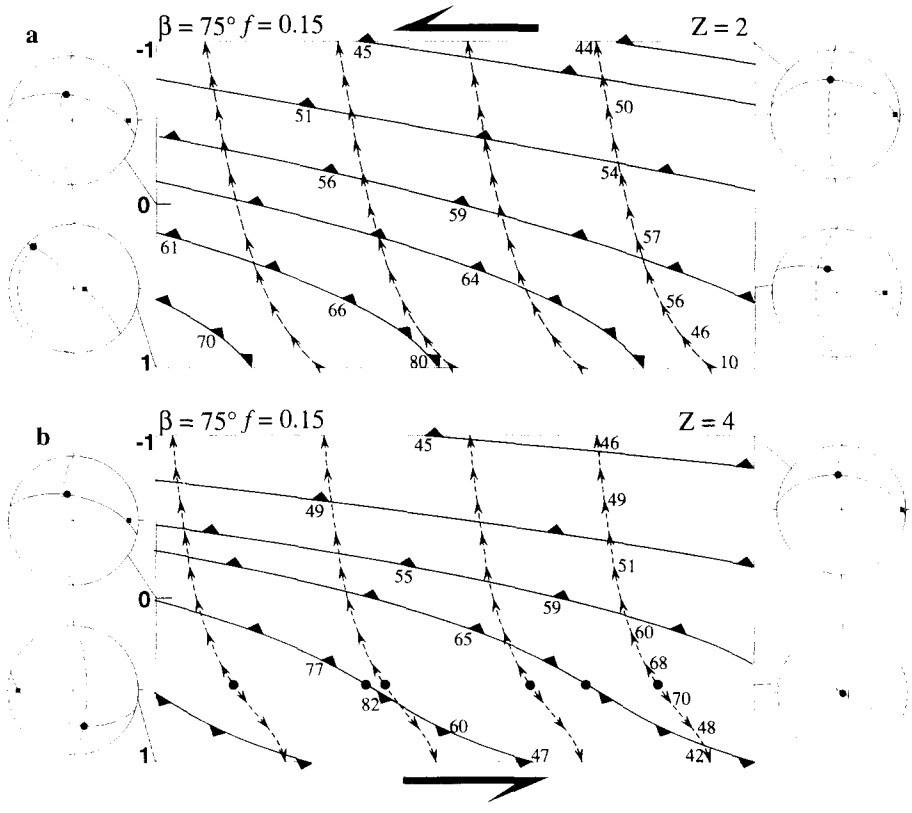


Fig. 13. 'Foliation' (solid lines) and 'lineation' (dotted lines) trajectory maps for two horizontal levels (a, $Z = 2$ and b, $Z = 4$) of the sinistral oblique transpression model with $f = 0.15$ and $\beta = 75°$. Equal-area, lower-hemisphere projections show the relationships between the vorticity vector (filled squares) and vorticity profile plane (dotted great circles) and the 'foliation' (solid great circles) and 'lineation' (filled circle) at selected points in the zone. Note the asymmetric fabric pattern and change from dip-slip to strike-slip kinematics across the zone at $Z = 2$ in (a). A similar pattern is observed in the Mylonite zone (Fig. 5).

vertical, toward the free surface. One advantage mentioned earlier of a 'stress–strain' model is that it is possible to check on its mechanical soundness quantitatively. We may therefore ask, for example: can a vertical transpression zone really have the thickness of the crust?

*Size and pressure in a transpression zone.* The pressure (i.e. the mean principal component of stress) in excess of lithostatic pressure which develops at the bottom centre of the zone ($Z = 0$) can be estimated from Jaeger's (1962, p. 142, section 40) equation 18. It is given, as a function of the viscosity, $\eta$, the rate of application of the 'press' component, $\phi$, and the normalized height, $Z_0$, of the free erosion surface by:

$$\Delta P \approx \tfrac{3}{2}\eta\phi Z_0^2. \qquad (10)$$

where $\Delta$ is to indicate that this is the value of an 'overpressure', i.e. pressure in excess of lithostatic. We can investigate equation (10) numerically. Taking, for example,

$$\eta = 10^{20} \text{ Pa s } (= 10^{19} \text{ poise}),$$
$$\phi = 10^{-14} \text{ s}^{-1}$$

(i.e. the zone loses 1/10th of its thickness in $10^{13}$ s, or 317,000 years), gives:

$$\Delta P = 1.5 \times Z_0^2 \times 10^6 \text{ Pa} = 0.015 \times Z_0^2 \text{ kbar}.$$

A zone with a width of 1 km, i.e. $h = 0.5$ km, and a height $z_0 = 5$ km ($Z_0 = 10$), would yield an overpressure (i.e. pressure above lithostatic) at the bottom of 150 MPa (1.5 kbar), which is plausible. But if we want $z_0 = 10$ km ($Z_0 = 20$) for a zone of the same 1 km width and same convergence rate, then $\Delta P = 600$ MPa (6 kbar), which seems high. Considering the square dependence on depth in equation (10), we see that a transpression zone with the height of the crust, e.g. $z_0 = 30$ km, needs to 'press' at a very low rate, be several-km thick, and/or contain material with anomalously low viscosities.

Generally, the development of a regional scale transpression zone, whether it involves the whole crust or not, is favoured where the temperature and fluid activities are high and the viscosity correspondingly low. Hutton & Reavy (1992) recently argued that the thickening of the crust expected from transpression in its tectonic sense could be responsible for the generation of magmas in the lower crust, at the base of several major shear zones. The present considerations suggest in addition that once these magmas have moved up and heated their hosts, and after erosion has removed part of the overburden, conditions become favourable for transpression, now in the structural sense, of the magmas and of their softened host rocks. Extrusion resulting from transpression, in addition to buoyancy, may therefore help to drive the upward migration of these magmas.

*Base of the transpression zone.* The present model assumes a rather unrealistic boundary condition at its base, $Z = 0$: specifically, the base is a perfectly lubricated planar surface. The base of a geological transpression zone cannot be like that. In view of the limit discussed above to the height of a transpressive zone, the relative displacement of the two walls has to be transferred to a non-transpressive mode at depth. For example, a wide, straight vertical transcurrent simple shear zone (i.e. non-transpressive) in the lower crust could be linked, through some sub-horizontal décollement zones, to vertical but curved zones in the upper crust: transcurrent transpression and transtension would arise in the upper crust, depending on the local orientation of the upper crustal zone with respect to that of the zone in the lower crust. Furlong & Hugo (1989) propose that such transfer along a horizontal décollement is happening eastward of the surface expression of the San Andreas Fault in northern California. Oblique transpression could occur in the vertical uppermost portion of a dipping, non-transpressive oblique shear zone, or in the top portion of a listric fault.

In either the transcurrent or the oblique case, the strain field close to the transfer level is not expected to resemble that in the ideal model used here. The model is therefore not applicable until the observation level is sufficiently above the base of the zone.

*Non-Newtonian rheologies*

If ductile transpression proceeds where the rates of deformation are slow, and the temperature and fluid activity are high, mechanisms such as stress-induced diffusion transfer, grain-boundary sliding, hydrolytic weakening, reaction softening, etc., may be important contributors to the deformation; Newtonian viscosity would then be a reasonable approximation. If the viscosity departs significantly from Newtonian, the strain field may further break down into subsidiary shear zones, as expected with high stress exponent rheologies, and into faults, such as the velocity discontinuities expected from ideally plastic behaviour. If the slip directions and slip senses along these zones are detectable, we propose that they should document the same variations in orientations of the extension directions and of the vorticity as those predicted by the viscous model.

*Incremental strain, accumulated strain and fabrics*

As exemplified in our presentation of the results, we believe that the relation of the foliation resulting from the accumulated strain to the instantaneous 'foliation' obtained in the model can be qualitatively predicted with our knowledge of the vorticity and vorticity number. First, as noted earlier, when the deformations are small, foliations and lineations should differ little from our instantaneous 'foliations' and 'lineations'. For large deformations, however, the non-zero vorticity means that the foliation and the lineations are progressively rotated from their initial orientations.

In progressive simple shear, such as found near the margins of all model transpression zones, the foliation and the lineation gradually rotate about the vorticity vector toward parallelism with the shear plane and with the shear direction, respectively. It is therefore straightforward to infer foliations and lineations from the incremental 'foliation' and 'lineation' in such parts of the zone.

Near the midplane of a transcurrent transpression zone, the symmetry of the deformation is monoclinic, regardless of whether the 'lineation' is parallel ($f > 0.236$) or perpendicular ($f < 0.236$) to the vertical vorticity vector. By reasons of symmetry, and considering that the sectional vorticity number is comparable to, but less than 1, it is safe to predict that the foliation will also rotate from its initial orientation, at 45° to the shear zone, toward parallelism with the shear zone. When the 'lineation' is horizontal, i.e. perpendicular to the vorticity vector, it should remain horizontal and rotate with the foliation toward parallelism with the shear direction. When the 'lineation' is vertical, and thus parallel to the vorticity vector, it should remain so during strain accumulation. An exception arises when $f$ is greater than 0.236 but close to it: the 'lineation' is vertical, but sufficient accumulated strain can lead to a horizontal maximum principal strain direction. Such a 'lineation switch' may be of little practical consequence since it occurs when $K \approx 0$, and therefore when the maximum extension direction is not expected to be expressed in the fabric as a lineation.

The literature offers no guidance to predict the evolution of the principal directions of accumulated strains for the general case of deformation with triclinic symmetry. We only speculate that the foliation and lineation would rotate about the vorticity vector, and since the sectional vorticity number, $W_k^s$, is $< 1$ everywhere, that such rotation would converge toward some stable direction rather than pulsate.

Inferring accumulated strain, and its consequent fabric, from the model incremental strain is thus not completely possible at present. More fundamentally, however, as discussed below, a transpressive zone is very likely to record more than the strain inherited from its transpressive history alone.

*Development and growth of a transpression zone and inherited fabric*

An actual ductile transpression zone cannot generally have been established, at some 'time zero', with its set width, a fixed 'press'/'trans' ratio $f$, a fixed obliquity $\beta$, a fixed viscosity inside and perfectly rigid walls at its margins. Instead, a transpression zone has to start as a shear zone. As shearing proceeds, the shear zone must then expand in size, and/or the material within it must soften sufficiently for transpression to become possible, somewhere near the surface or some other 'escape' boundary. And even after transpression has started, there is the possibility that the zone continues to increase in size, change in $f$, change in obliquity, etc. Thus, its

final width, and the several components of its total strain field are really only the integrated results of a long, and probably varied, history. The actual fabric observed in a transpression zone will therefore record more than the transpressive part of its history: it should record the history of its progressive development into a shear zone and then into a transpression zone. Even within an established zone, Treagus & Treagus (1992) have recently argued that transected folds within transpression zones could be best explained by a progressive decrease in the 'press'/'trans' ratio throughout the history of the zone. These authors also remind readers, in the context of transpression, that the relationship of fabrics with strain is not uniquely prescribed. Accordingly, the final fabric pattern observed in the field has many reasons to differ from that in our simple model in ways that could not be resolved by simply tracking strain increments into a finite strain within a set ductile transpression zone.

## CONCLUSIONS

The increasing evidence for tectonic transpression and for structural transpressive deformation suggests that geologists should examine the consequences of ductile transpression in more detail. While actual field examples of ductile transpression are likely to be more complicated than the model zones presented here, they should nevertheless record the consequences of heterogeneous deformation which the model predicts. These consequences include systematic variations in lineation directions across the zone, and local departures of the fabric symmetry from the monoclinic symmetry expected in progressive simple shear. The Archean Larder Lake–Cadillac deformation zone, in the Canadian Shield, and the Mid-Proterozoic Mylonite Zone, in the Sveconorwegian orogenic province, exhibit fabric patterns and fabric symmetries which match several of the model predictions.

Dynamic models such as the one used here provide some quantitative physical constraints on the rates, sizes and viscosities of transpressive systems. They suggest in particular that ductile transpression on a regional scale may be limited in depth to a few kilometres unless special geological circumstances provide for several-km wide zones of low viscosities. In the absence of such circumstances, transpressive motion in the upper crust must be transferred to non-transpressive motion at depth.

General heterogeneous velocity fields are expected under many conditions other than just transpression. The method used here to calculate vorticity and spin should be generally applicable, and the triclinic symmetry of the deformation and of the consequent fabric is likely to be a general feature rather than an exception. The consequences of triclinic deformation on fabric evolution needs to be explored further.

*Acknowledgements*—This work was supported by Operating and Lithoprobe grants from the National Science and Engineering Research Council of Canada, and research support from Erindale College, University of Toronto, to the authors. Thorough reviews of the manuscript by W. M. Schwerdtner and F. W. Vollmer, as well as comments by W. D. Means, P. F. Williams and Jeremy Brett helped improve the presentation significantly. W. M. Schwerdtner has, over the years, provided a continuing education in strain theory and strain models to P.-Y. F. Robin, and a presentation by, and discussion with, D. J. Sanderson gave both authors the initial encouragement to do the present work. Lithoprobe publication No. 451.

## REFERENCES

Borradaile, G. & Spark, R. 1991. Deformation of the Archean Quetico–Shebandowan subprovince boundary in the Canadian Shield near Kashabowie, northern Ontario. *Can. J. Earth Sci.* **28**, 116–125.

Borradaile, G., Sarvas, P., Dutka, R., Stewart, R. & Stubley, M. 1988. Transpression in slates along the margin of an Archean gneiss belt, northern Ontario—magnetic fabrics and petrofabrics. *Can. J. Earth Sci.* **25**, 1069–1077.

Burgmann, R. 1991. Transpression along the southern San Andreas Fault, Durmid Hill, California. *Tectonics* **10**, 1152–1163.

Cruden, A. R. 1991. Syntectonic plutons in the Larder Lake–Cadillac Deformation Zone: Implications for the timing of late Archean deformation in the S.W. Abitibi Belt. In: *Abitibi–Grenville Transect Workshop, Lithoprobe Report* 25. University of British Columbia, 139–142.

D'Lemos, R. S., Brown, M. & Strachan, R. A. 1992. Granite magma generation, ascent and emplacement within a transpressional orogen. *J. geol. Soc. Lond.* **149**, 487–490.

Furlong, K. P. & Hugo, W. D. 1989. Geometry and evolution of the San Andreas Fault Zone in northern California. *J. geophys. Res.* **94**, 3100–3110.

Hanmer, S. 1981. Tectonic significance of the northeastern Gander Zone, Newfoundland: an Acadian ductile shear zone. *Can. J. Earth Sci.* **18**, 121–135.

Harland, W. B. 1971. Tectonic transpression in Caledonian Spitsbergen. *Geol. Mag.* **108**, 27–42.

Hodgson, C. J. & Hamilton, J. V. 1989. Gold mineralization in the Abitibi greenstone belt: End stage result of Archean collisional tectonics? *Econ. Geol. Monogr.* **6**, 86–100.

Hudleston, P. J., Schultz-Ela, D. & Southwick, D. L. 1988. Transpression in an Archean greenstone belt, northern Minnesota. *Can. J. Earth Sci.* **25**, 1060–1068.

Hutton, D. H. W. 1987. Strike slip terranes and a model for the evolution of the British and Irish Caledonides. *Geol. Mag.* **124**, 405–425.

Hutton, D. H. W. & Reavy, R. J. 1992. Strike-slip tectonics and granite petrogenesis. *Tectonics* **11**, 960–967.

Jackson, S. L. & Fyon, J. A. 1991. The western Abitibi Subprovince in Ontario. In: *Geology of Ontario. Ontario geol. Surv. Spec. Vol.* **4**, Pt. 1, 405–482.

Jackson, S. L., Sutcliffe, R. H., Ludden, J. N., Hubert, C., Green, A. G., Milkereit, B., Mayrand, L., West, G. F. & Verpaelst, P. 1990. Southern Abitibi Greenstone Belt: Archean crustal structure from seismic reflection profiles. *Geology* **18**, 1086–1090.

Jaeger, J. C. 1962. *Elasticity, Fracture and Flow*. John Wiley & Sons, New York.

Jensen, L. S. 1985. Synoptic mapping of the Kirkland Lake–Larder Lake areas, district of Tamiskaming. *Ontario geol. Surv. Misc. Pap.* **126**, 112–120.

Lin, S. & Williams, P. F. 1992. The geometrical relationship between the stretching lineation and the movement direction of shear zones. *J. Struct. Geol.* **14**, 491–497.

McKenzie, D. 1979. Finite deformation during fluid flow. *Geophys. J. R. astr. Soc.* **58**, 689–715.

Means, W. D., Hobbs, B. E., Lister, G. S. & Williams, P. F. 1980. Vorticity and non-coaxiality in progressive deformations. *J. Struct. Geol.* **2**, 371–378.

Park, R. G., Åhäll, K.-I. & Boland, M. P. 1991. The Sveconorwegian shear-zone network of SW Sweden in relation to mid-Proterozoic plate movements. *Precambrian Res.* **49**, 245–260.

Ramsay, J. G. & Huber, M. I. 1983. *The Techniques of Modern Structural Geology, Volume 1: Strain Analysis*. Academic Press, London.

Ramsay, J. G. & Graham, R. H. 1970. Strain variation in shear belts. *Can. J. Earth Sci.* **7**, 786–813.

Ramsay, J. G. & Graham, R. H. 1970. Strain variation in shear belts. *Can. J. Earth Sci.* **7**, 786–813.
Ratliff, R., Morris, A. & Dodt, M. 1988. Interaction between strike-slip and thrust-shear: deformation of the Bullbreen Group, Central-Western Spitsbergen. *J. Geol.* **96**, 339–349.
Ratschbacher, L. 1986. Kinematics of austro-alpine cover nappes: changing translation path due to transpression. *Tectonophysics* **125**, 335–356.
Robert, F., 1989. Internal structure of the Cadillac tectonic zone southeast of Val d'Or, Abitibi greenstone belt, Quebec. *Can. J. Earth Sci.* **26**, 2661–2675.
Robin, P.-Y. F. & Cruden, A. R. 1991. Strain fabric patterns in ideally ductile transpressive zones and in a possible Archean prototype: the Larder Lake Break. *Geol. Soc. Am. Abs. w. Prog.* **23**, A177.
Sanderson, D. J. & McCross, A. M. 1991. Modelling of transpression/transtension. *Geol. Ass. Can. Prog. w. Abs.* **16**, A110.
Sanderson, D. J. and Marchini, W. R. D. 1984. Transpression. *J. Struct. Geol.* **6**, 449–458.
Schmeling, H., Cruden, A. R. & Marquart, G. 1988. Finite deformation in and around a fluid sphere moving through a viscous medium: implications for diapiric ascent. *Tectonophysics* **149**, 17–34.
Schwerdtner, W. M. 1989. The solid-body tilt of deformed paleohorizontal planes: application to an Archean transpression zone, southern Canadian Shield. *J. Struct. Geol.* **11**, 1021–1027.
Stephens, M. B., Wahlgren, C.-H., Weijermars, R. & Cruden, A. R. 1993. Sinistral transpressive deformation along the Mylonite Zone, Sveconorwegian (=Grenvillian) Province, southwestern Sweden. *Terra Nova* **5**, Abs. Suppl. 1, 321.
Stott, G. M., Sanborn-Barrie, M. & Corfu, F. 1987. Minor transpressional events recorded across Archean subprovince boundaries in north-western Ontario. *Can. Prog. w. Abs.* **12**, 24.
Sylvester, A. G. & Smith, R. R. 1976. Tectonic transpression and basement-controlled deformation in San Andreas Fault zone, Salton Trough, California. *Bull. Am. Ass. Petrol. Geol.* **60**, 2081–2101.
Toogood, D. J. & Hodgson, C. J. 1986. Relationship between gold deposits and the tectonic framework of the Abitibi greenstone belt in the Kirkland Lake-Larder area. *Ontario geol. Surv. Misc. Pap.* **130**, 4–15.
Treagus, S. H. & Treagus, J. E. 1992. Transected folds and transpression: how are they associated? *J. Struct. Geol.* **14**, 361–367.
Truesdell, C. 1953. Two measures of vorticity. *J. Rational Mech. Anal.* **2**, 173–217.
Wilkinson, L. & Cruden, A. R. 1992. Post-Timiskaming structural history of the Kirkland Lake area. In: *Abitibi–Grenville Transect Workshop, Lithoprope Report* 33. University of British Columbia, 61–64.
Williams, H. R., Stott, G. M., Thurston, P. C., Sutcliffe, R. H., Bennet, G., Easton, R. M. & Armstrong, D. K. 1991. Tectonic evolution of Ontario: Summary and synthesis. In: *Geology of Ontario. Ontario geol. Surv. Spec. Vol.* **4**, Pt. 2, 1255–1332.

## APPENDIX A

## THE 'PRESS' COMPONENT OF THE VELOCITY GRADIENT TENSOR

Jaeger (1962, section 40, pp. 140 & ff., equation 16) gives the solution to the extrusion problem as a velocity field. Replacing Jaeger's parameter $V_0$ by $\varphi h$, and switching from his $x\,y$ co-ordinates to our $z\,y$ co-ordinates, his equation (16) for the components of the velocity field becomes:

$$v = \tfrac{1}{2}\varphi \frac{y(h^2 - 3y^2)}{h^2} \tag{A1a}$$

$$w = \tfrac{3}{2}\varphi \frac{z(h^2 - y^2)}{h^2}. \tag{A1b}$$

The only non-zero derivatives are easily calculated as:

$$\frac{\partial w}{\partial z} = -\frac{\partial v}{\partial y} = \frac{3}{2}\varphi \frac{(h^2 - y^2)}{h^2} \tag{A2a,b}$$

$$\frac{\partial w}{\partial y} = -3\varphi \frac{yz}{h^2}. \tag{A2c}$$

Replacing $y/h$ and $z/h$ by $Y$ and $Z$ yields the part of equation (1) which is associated with the extrusion.

## APPENDIX B

## EXTERNAL AND INTERNAL VORTICITY

In order to evaluate the difference between the internal and the external vorticity, it is first necessary to evaluate how the principal directions of strain rotate along the path of a particle (e.g. see Means *et al.* 1980). Since, for given values of $Y$ and $Z$, the strain is the same for all values of $X$, we only need to consider the variations of orientation as a function of the $Y$ and $Z$ co-ordinates.

*Rotation of the principal directions of strain between two adjacent points in the zone*

Let us call $V(Y, Z)$ the $3 \times 3$ orthogonal matrix consisting of the direction cosines of the principal directions of the strain rate tensor at point $(Y, Z)$. As discussed in the main text, $V$ is calculated numerically with TRPR.M and yields the directions of 'foliations' and 'lineations' at each point. Consider now an adjacent point $(Y + \mathrm{d}Y, Z + \mathrm{d}Z)$. Its principal directions differ by a small rotation, $\mathrm{d}\alpha$, from those at $(Y, Z)$:

$$V(Y + \mathrm{d}Y, Z + \mathrm{d}Z) = (I + \mathrm{d}\alpha)V\,(Y, Z). \tag{B1}$$

As long as $(\mathrm{d}Y, \mathrm{d}Z)$ is small and the rotation is therefore also small, the matrix $\mathrm{d}\alpha$ is antisymmetric. It can be decomposed into:

$$\mathrm{d}\alpha = \frac{\partial \alpha}{\partial Y}\mathrm{d}Y + \frac{\partial \alpha}{\partial Z}\mathrm{d}Z. \tag{B2}$$

Since we have not derived analytical expressions for $V$, the partial derivatives must be evaluated numerically, e.g. by finite differences:

$$\frac{\partial \alpha}{\partial Y} = \frac{1}{2\Delta Y}[V(Y + \Delta Y, Z) - V(Y - \Delta Y, Z)]V^{\mathrm{T}}(Y, Z) \tag{B3a}$$

and

$$\frac{\partial \alpha}{\partial Z} = \frac{1}{2\Delta Z}[V(Y, Z + \Delta Z) - V(Y, Z - \Delta Z)]V^{\mathrm{T}}(Y, Z). \tag{B3b}$$

To obtain equation (B3) from (B1), we have used the fact that $V$ is an orthogonal matrix, and therefore its inverse equals its transpose. The spans $\Delta Y$ and $\Delta Z$ used to calculate the finite differences may be adjusted, depending on how rapidly the principal directions rotate.

*Changes in normalized co-ordinates of a particle during a strain increment*

The changes in relative position $(Y, Z)$, of a particle during a unit time must now be calculated. The half-width of the zone changes by

$$\frac{\mathrm{d}h}{\mathrm{d}t} = -\varphi h \tag{B4}$$

and since $Y = y/h$,

$$\frac{\mathrm{d}Y}{\mathrm{d}t} = \frac{1}{h}\frac{\mathrm{d}y}{\mathrm{d}t} - \frac{y}{h^2}\frac{\mathrm{d}h}{\mathrm{d}t} = \frac{v}{h} + \varphi\frac{y}{h}$$

or, using equation (A1a) to replace $v$,

$$\frac{\mathrm{d}Y}{\mathrm{d}t} = \frac{1}{2}\varphi\frac{y(y^2 - 3h^2)}{h^3} + \varphi\frac{y}{h} = -\frac{1}{2}\varphi Y(1 - Y^2). \tag{B5a}$$

Similarly,

$$\frac{\mathrm{d}Z}{\mathrm{d}t} = \frac{3}{2}\varphi\frac{z(h^2 - y^2)}{h^3} + \varphi\frac{z}{h} = \frac{1}{2}\varphi Z(5 - 3Y^2). \tag{B5b}$$

Replacing $\varphi$ by $\gamma f$, we finally get

$$\frac{\mathrm{d}Y}{\mathrm{d}t} = -\frac{\gamma}{2}fY(1 - Y^2) \tag{B6a}$$

$$\frac{\mathrm{d}Z}{\mathrm{d}t} = \frac{\gamma}{2}fZ(5 - 3Y^2). \tag{B6b}$$

The rotation tensor, $\rho$, for the principal directions of strain around a particle during a unit of time is therefore obtained by combining equations (B2) and B6):

$$\rho = \frac{d\alpha}{dt} = \frac{\gamma}{2} f\left(-Y(1 - Y^2)\frac{\partial \alpha}{\partial Y} + Z(5 - 3Y^2)\frac{\partial \alpha}{\partial Z}\right) \quad \text{(B7)}$$

in which, we recall, rotation matrices $\partial\alpha/\partial Y$ and $\partial\alpha/\partial Z$ are evaluated numerically (equation B3). Means *et al.* (1980) proposed to call $\rho$ the *spin* tensor. It can be directly compared with $\omega$, the antisymmetric part of the velocity gradient tensor (equation 3). The internal vorticity is described by $(\omega - \rho)$. The magnitude of the corresponding rotation can be calculated in the same manner as that of the vorticity. Numerically, because $\rho$ is only approximately antisymmetric, the magnitude, $|P|$, is calculated by

$$|P| = \sqrt{-(\rho_{yz}\rho_{zy} + \rho_{zx}\rho_{xz} + \rho_{xy}\rho_{yx})}. \quad \text{(B8)}$$

Rather than calculating $\rho$ within TRPR.M, a separate program, VORTI.M, was written to calculate and compare the magnitudes of $|P|$ and $|\Omega|$ at any point. While the spin magnitude was less than 10% of the external vorticity almost everywhere, the ratio $|P|/|\Omega|$ does reach significantly higher values, with a maximum, as seen on the transverse profile, which depends on the 'press'/'trans' ratio, $f$, and the level $Z$. The position of that maximum was for values of $|Y|$ ranging from 0.15 to 0.4. For realistic values of $f$ ($f < 0.25$), and of $Z(2 < Z < 8)$, the maximum value of the $|P|/|\Omega|$ ratio varied from 10% (for $f = 0.1$, $Z = 2$) to 25% (for $f = 0.25$, $Z = 2$). Although 25% is not negligible, we chose to ignore $\rho$ in calculating the vorticity because of the simplification that that provided in the calculation of the sectional vorticity number (equation 9) and in the presentation of the results.